Helvetica Physica Acta,
Vol. 56 (1983) 331-346

0018-0238/83/010331-16$1.50+0.20/0

THE EFFECT OF HYDROSTATIC PRESSURE ON SHALLOW AND DEEP IMPURITY STATES IN SEMICONDUCTORS

S. Porowski and W. Trzeciakowski

High Pressure Research Center "Unipress"
Polish Academy of Sciences
01-142 Warsaw, Poland

The influence of hydrostatic pressure on various contributions to the impurity potential is discussed. The pressure dependence of impurity states is described for the potentials containing the slowly-varying term, the short-range term, and both of these terms. The effect of pressure on the impurity-lattice coupling is discussed. All the above considerations are illustrated with appropriate experimental results.

1. Introduction

The main effect introduced by the hydrostatic pressure applied to the crystal consists in the change of the lattice constant a_o. As the relative magnitude of this change is usually small /e.g. for CdTe at 1 GPa $\Delta a_o/a_o = .007$/ we can expect that most of the crystal parameters will vary linearly with pressure. From the theoretical point of view high pressure is the simplest method for modifying the crystal structure and the energy spectrum of electrons. Temperature variation, for instance, leads to a change of the lattice vibrations which, in turn, influence the electronic energy spectrum in a very complicated way. Alloying, even in the simplest virtual-crystal approximation, introduces a disorder potential. Application of the external magnetic and electric fields lowers the symmetry of the system.

The impurity states control most of the crystal properties, therefore their investigation has been one of the main areas of solid-state physics. Practically all experiments which yield the information about the impurity states can be performed under hydrostatic pressure. In that way we obtain an additional variable parameter which allows to examine various theoretical mo-

dels of impurity states.

Before we discuss the influence of pressure on impurities, let us briefly comment on two experimental techniques, used in high-pressure studies of impurity states. Very high pressures are relatively easy to achieve in very small volumes. This is the case of the diamond anvils /Fig.1/ where the metal gasket is squeezed by two truncated, brilliant-cut diamonds. Tiny hole in the gasket filled with some pressure-transmitting liquid contains a small sample of the examined crystal. The pressure is measured by a microscopic piece of a ruby/the luminescence line of chromium impurity shifts with pressure/. Such anvils are mainly used for optical experiments and they allow to obtain hydrostatic pressures up to 50 GPa. The experiments which require more space may be performed in piston-cylinder cells /Fig.2b/ or the cells connected to a gas compressor /Fig.2a/.

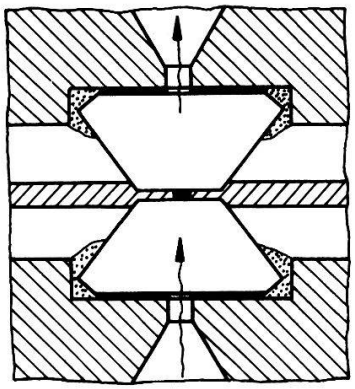

Fig.1. Diamond anvils used for optical [2] or X-ray [3] experiments.

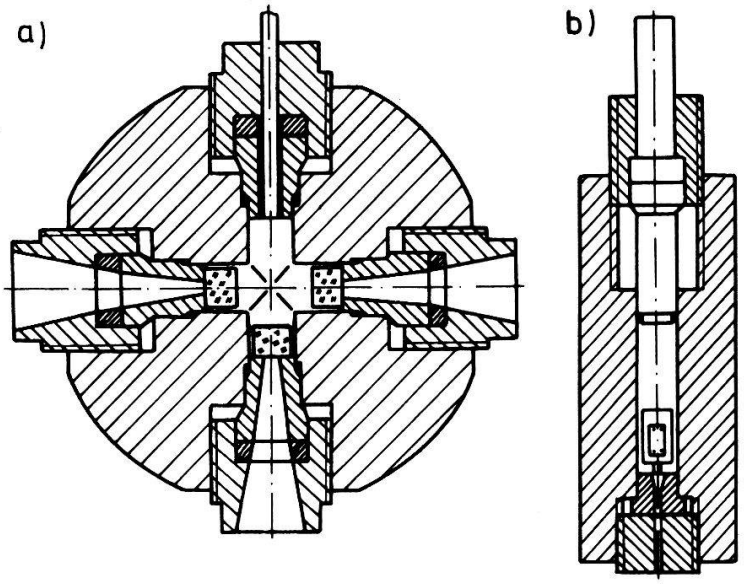

Fig.2. High-pressure "Unipress" cells [1]: a/ optical cell connected to a gas compressor by a capillary b/ clamp-cell with liquid for pressures up to 2.7 GPa.

Here the maximum pressure usually does not exceed 3 GPa but all techniques for studying impurity states /absorption and luminescence, photoconductivity, Raman scattering, EPR or ENDOR, thermoelectric and galvanomagnetic effects, DLTS etc/ can be applied in appropriate pressure cells. The available temperature range is also very broad /from liquid helium to 2000 K/ and high magnetic fields are easily applied.

2. The influence of pressure on the impurity potential.

In the one-electron approximation the impurity states are obtained as the eigenvectors of the Hamiltonian $H = p^2/2m_o + V_{cr} + V_{imp}$ where V_{cr} is the periodic crystal potential and V_{imp} is the total potential introduced by the impurity. In general, V_{imp} contains the long-range Coulomb potential /due to the effective charge of the defect/ the short-range potential /due to the difference in the host and impurity cores/, and the potential produced by the lattice deformation brought about by the impurity. Each term of the potential should be properly screened. All these terms are affected by the hydrostatic pressure and we shall now briefly discuss this dependence.

The influence of pressure on V_{cr} /through the modification of the lattice constant/ leads to the pressure dependence of the band structure of the perfect crystal. In narrow-gap materials like InSb the hydrostatic pressure can increase the gap /and therefore the effective mass/ at the Γ point by the factor of 3 which strongly affects shallow impurity states [4,5]. The influence of pressure on the band structure can be studied theoretically [6] but the experimental knowledge is in most semiconductors restricted only to some estimates of the pressure coefficients of the conduction band minima [7]. Therefore several simplified models of the conduction band density of states /and its pressure dependence/ have been used /Fig.3/. In Ref.4 for the purpose of studying shallow impurity states it was assumed that the conduction band consists of a parabolic minimum, moving upwards as the pressure increases /the mass in this minimum increases with pressure/, and the "bulk of the band" in-

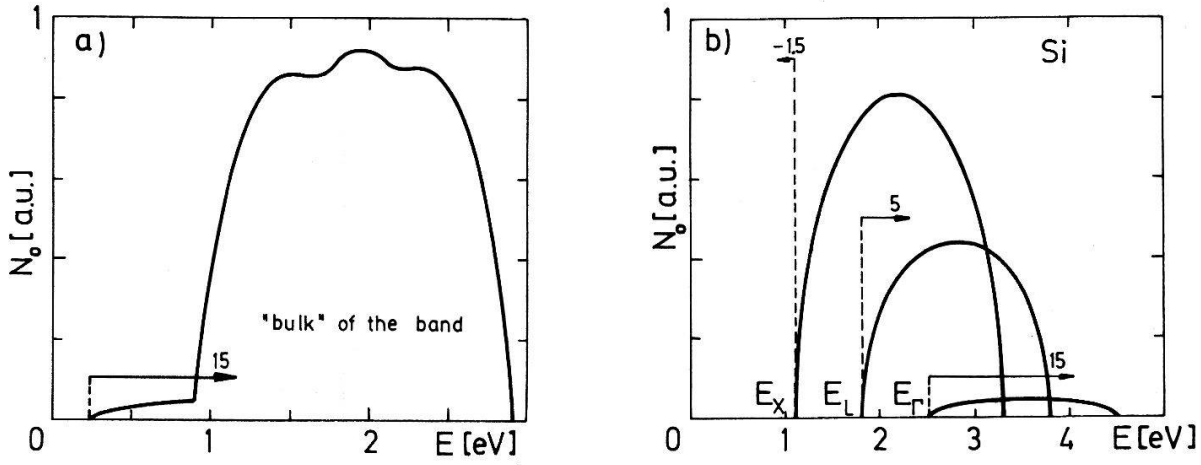

Fig.3. Two simplified models of the pressure variation of the conduction band density of states: a/parabolic minimum in InSb moving up towards the immobile "bulk of the band" b/ three elliptic contributions associated with Γ, L, and X minima in Si, moving with various pressure coefficients /indicated by arrows/

sensitive to the pressure /Fig.3a/. In Ref.8 it was assumed that each minimum of the conduction band contributes an elliptic term to the total density of states, each ellipse possessing a different pressure coefficient /Fig.3b/.

The influence of pressure on the long-range Coulomb potential arises from the pressure dependence of screening, mainly by free carriers. Pressure induced change of the band gap leads to a change in the mass and concentration of free carriers, which can cause strong modification of screening.

The short-range core potential is unaltered by small changes of the lattice constant. However, in the presence of free carriers it is always accompanied by a long-range potential [9] which can vary with pressure.

The potential produced by the lattice deformation around the impurity may be substantially modified by the application of the hydrostatic pressure. This modification may be due to the difference of the local compressibility of the lattice around the impurity from that in the perfect crystal.Such difference was often reported in the pressure studies of crystal-field splittings of deep, atomic-like impurity levels [10,11]. Moreover, as will be discussed in Sec.4, the hydrostatic pressure may cause a complete change of configuration of the atoms surrounding the impurity as a result of the pressure induced crossing of the states coupled to the lattice.

3. The effect of pressure on the electronic impurity states.

The commonly adopted terms "shallow" and "deep" impurities are not very precize because there are several minima in the band so that the "depth" of the state depends on which minimum we refer it to. Therefore, we should rather distinguish between the states dominated by the long-range or by the highly-localized impurity potential. It also turns out that the pressure dependence of impurity states is different in these two cases. We shall first discuss the case of the slowly-varying potential described by the Effective-Mass Theory. Then we shall examine the simple one-site-one-band model introduced by Koster and Slater for the localized impurity potential. Finally we consider an intermediate case when both parts of the potential are important /Trzeciakowski-Krupski model/.

3.1 Slowly-varying potential.

When the impurity potential is slowly-varying in one elementary cell the wave function of the bound carrier may be constructed from the Bloch functions $\psi_{n\vec{k}}(\vec{r})$ with $\vec{k}$ vectors restricted to a small region of the Brillouin

zone /around the minimum of the band/. For the Coulomb potential $-Ze^2/\varepsilon r$ we obtain the hydrogenic-like spectrum of impurity states under each parabolic minimum

$$E_n^i = \frac{-m^* Z^2 e^4}{2n^2 \hbar^2 \varepsilon^2} + E_o^i \quad , \tag{1}$$

$$\psi_{nlm}^i(\vec{r}) = \phi_{nlm}(\vec{r}) \cdot \psi_o^i(\vec{r}) \quad , \tag{2}$$

where E_o^i and $\psi_o^i(\vec{r})$ are the energies and wave functions from the i-th minimum while $\phi_{nlm}(\vec{r})$ are the hydrogenic-like envelope functions with the effective Bohr radii $a_n = n\hbar^2\varepsilon/Zm^*e^2$. The change of E_n^i with pressure due to the $m^*(p)$ dependence is usually quite small compared to $E_o^i(p)$ variation. Therefore it is evident that such impurity states will move with pressure similarly to the minimum they are attached to.

The change of the Bohr radii with pressure may lead to the pressure induced Mott transition. It should happen when

$$a_n \leqslant 0.26\, n_s^{-1/3} \quad , \tag{3}$$

where n_s is the shallow impurity concentration. If, as it is often the case, the Mott transition is studied as a function of the magnetic field, high pressure will shift the field at which the transition occurs /Fig.4/.

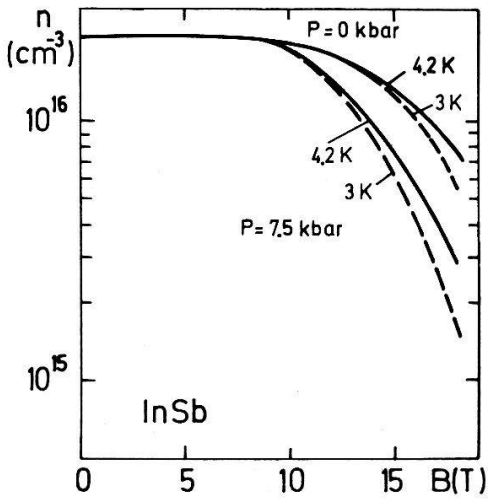

Fig.4. The influence of pressure /and temperature/ on the magnetic-field induced Mott transition in n-InSb [12] .

The optical investigations of shallow impurity states also used to be performed in high magnetic fields, because at $\vec{B} = 0$ the condition (3) was usually not satisfied, especcially in narrow-gap materials. The pressure dependence of the intra-impurity magnetooptical transitions for four shallow do-

nors in InSb is shown on Fig.5b. It was obtained from far-infrared photoconductivity measurements [5] /Fig.5a/. For a wider-gap semiconductor such measurements could be performed without the magnetic field.

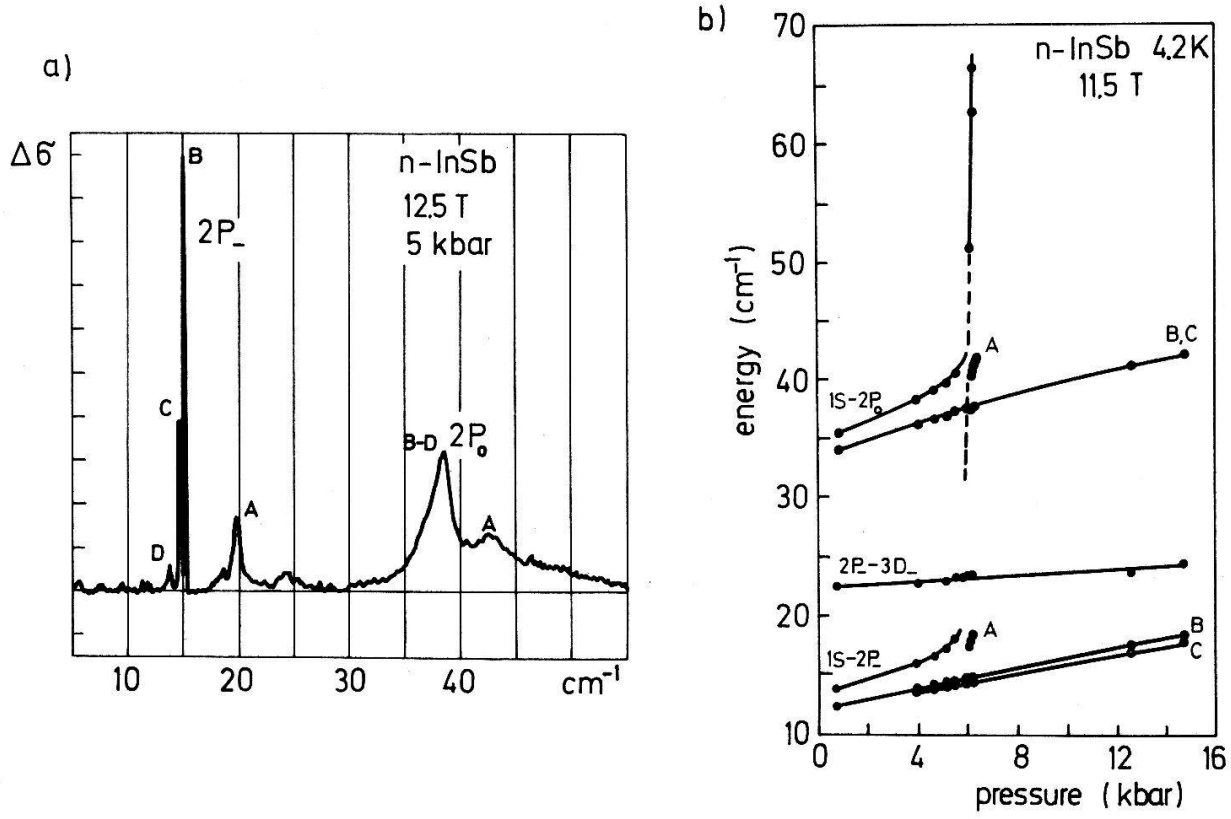

Fig.5. a/ the example of the photoconductivity spectrum revealing the $1S \rightarrow 2P_0$ transitions for four shallow donors /A, B, C, and D/ in InSb
b/ the pressure dependence of intra-impurity transitions suggesting the level crossing for the donor A.

The existence of several lines in the photoconductivity spectra and their departure from the hydrogenic-like behaviour is due to the chemical shift of shallow donors caused by their different central-cell potentials /see Sec.3.3/. The abrupt change of the pressure coefficient of the A-donor lines on Fig.5b most probably arises from its crossing with another level of the same symmetry /often attributed to the L-minimum as its pressure coefficient coincides with that of the L-minimum/. This L-like level was independently found in transport measurements [13] and its magnetic-field and pressure dependence was the same as in magnetooptics. However, its energetic distance from the L-minimum suggests that it cannot be properly described within the Effective Mass Theory. We shall return to this level in Sec.4.2

3.2 Highly-localized potential.

Assuming the potential to be localized in one elementary cell and taking into account only one band we may characterize the impurity by a single matrix element V_o /between the Wannier functions centered at the impurity site [14]/. Localized /or resonant/ impurity levels E_{imp} are given by the condition

$$\mathcal{P}\int \frac{N_o(E')\,dE'}{E_{imp} - E'} = \frac{1}{V_o} \qquad (4)$$

where $N_o(E')$ denotes the density of states in the considered band and $\mathcal{P}$ stands for the principal value. The pressure dependence of E_{imp} follows from the pressure dependence of $N_o(E')$. Adopting, for instance, the model presented on Fig.3b we get the pressure coefficient of the impurity level as a weighted average of the Γ, L, and X subbands [8] /Fig.6/. This coefficient depends on the position of the level. In other words, the pressure variation of the level is nonlinear for deep states /Fig.7a/. However, quite often the range of pressures available may be too small to observe this nonlinearity.

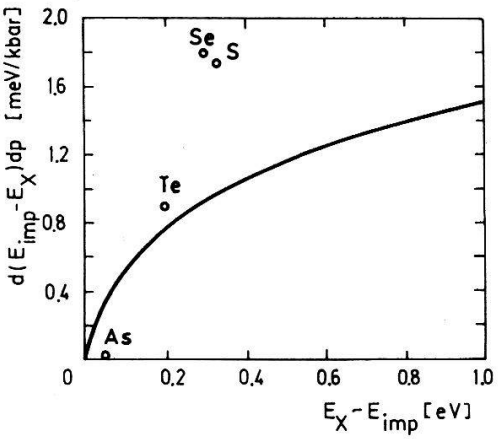

Fig.6. The pressure coefficient from the one-site-one-band model for Si /see Fig.3b/. The circles denote the experimental results from Ref.15.

The example of the experimental results interpreted with the Koster-Slater model is given on Fig.7. The measurements of the Hall and Shubnikov-de Haas effects [8] /which yield the pressure dependence of the free-carrier concentration/ were performed on InSb doped with S and Se, at various temperatures. The pressure-induced shift of the resonant impurity states with respect to the Γ subband affects the free-carrier concentration in this subband. The Koster-Slater model yields not only the energies, but also the half-widths of the resonant states /Fig.7a/. This enables to calculate the n(p) dependences /solid

lines on Fig.7b/ which fit the experimental results quite well /for a given impurity the only fitting parameter is V_o/.

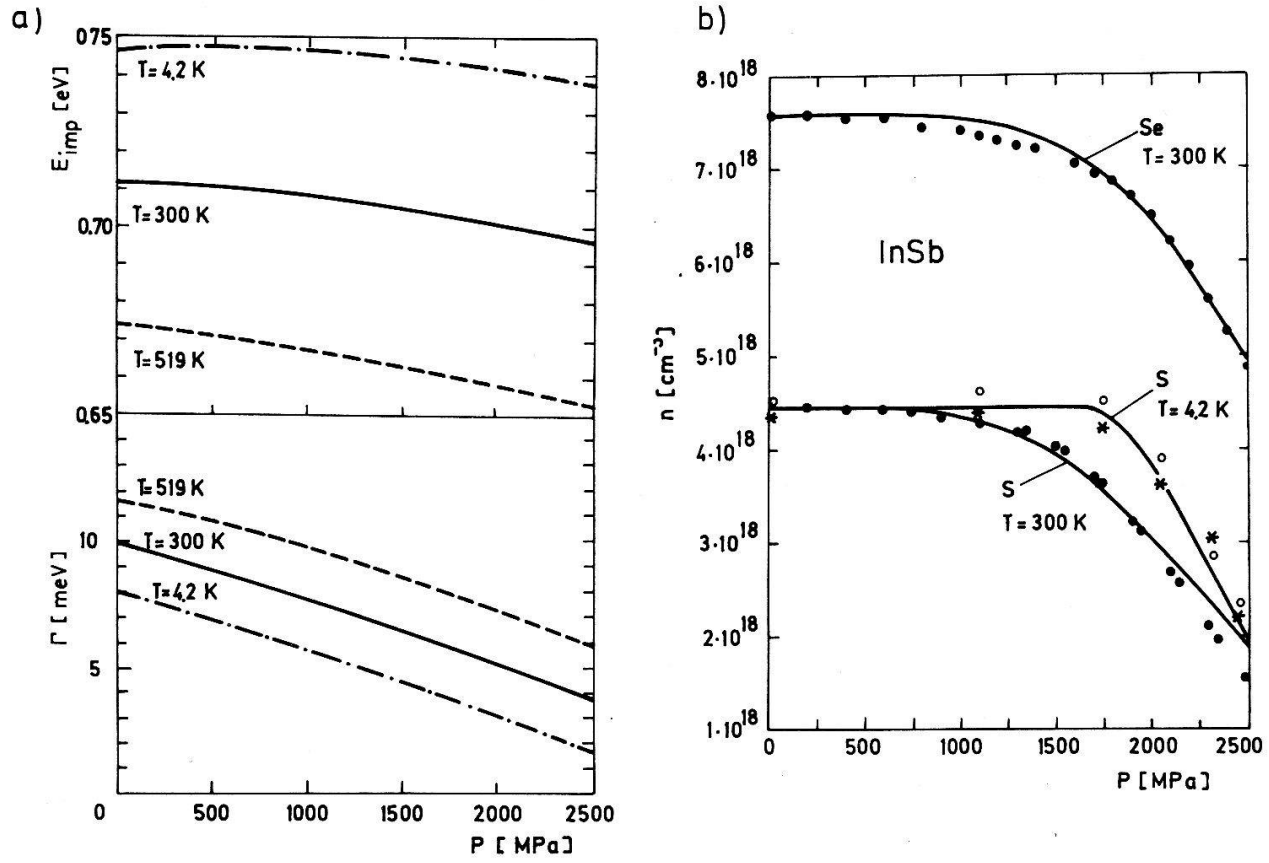

Fig.7. a/ theoretical pressure dependence of the energies and widths of the resonant states of S in InSb for various temperatures /energies are measured from the top of the valence band/ b/ results of the Hall (•, ∘) and Shubnikov-de Haas (*) measurements, interpreted with the Koster-Slater model /solid lines/.

The one-site-one-band model gives only one discrete /or resonant/ impurity state in the band. The multisite extension of this model [16] yields two states in the conduction band and well accounts for the observed composition /or pressure/ dependence of the nitrogen traps in $GaAs_{1-x}P_x$.

Many of the observed chemical trends in deep impurity energies in various semiconductors can be interpreted in the framework of the tight-binding model of Hjalmarson et al [17]. In this model the pressure dependence arises from the change in the interatomic transfer matrix elements with bond length. The pressure coefficients of deep levels in Si predicted by this model have the same order of magnitude as those obtained from DLTS measurements by Jantsch et al [15]. Their results for chalcogen donors are denoted by circles on Fig.6. The pressure coefficients increase with the depth of the state.

The authors argue that the value of the pressure coefficient may serve as a criterion for distinguishing between "deep" /highly localized/ and "shallow" /hydrogenic-like/ impurity states. However, from Fig.6 we see that within the Koster-Slater model, highly-localized states may have the pressure coefficient of a particular minimum, if only they lie close enough to this minimum.

Anyway, in case of chalcogen donors in Si we may regard As as shallow, S and Se as deep states. Jantsch and coworkers believe that Te state is on the borderline between deep and shallow i.e. in this case both the highly-localized and Coulomb potentials may be important.

3.3 Highly-localized and Coulomb potential.

The ground states of shallow impurities revealed large deviations from the predictions of the Effective Mass Theory. This was attributed to the presence of short-range /central-cell/ potentials arising mainly from the difference of the host and impurity cores. For a hydrogenic-like ground state the probability of finding the carrier in the central cell $|\psi_{100}(0)|^2 a_o^3/4$ is proportional to $(m^*)^3$. It is thus evident that the hydrostatic pressure, which can change m^* substantially, may largely increase the role of the central-cell potential.

In the model developed by Trzeciakowski and Krupski [4] the density of states in the band was taken as on Fig.3a. The localized impurity potential and the "bulk of the band" are described by one fitting parameter which can be replaced by the shift of the ground level $\tilde{E}_o = (E_{imp} - E_1)/E_1$ at zero pressure /$|E_1|$ is the effective rydberg/. The pressure dependence of E_{imp} calculated for various $\tilde{E}_o$ in InSb and CdTe is shown on Fig.8. The "collapsing" of the ground-state energy with pressure is much weaker for CdTe due to a much weaker $m^*(p)$ dependence in this material. However, much larger values of $\tilde{E}_o$ can be expected in CdTe than in InSb. The results of high-pressure photoconductivity measurements in InSb and GaAs [5] seem to agree with the predictions of this model.

Another interesting prediction of the considered theory is the pressure dependence of the wave function at the impurity site /Fig.9/. The value of $|\psi(0)|^2$ can be inferred from the results of EPR and ENDOR experiments, as it determines the hyperfine splittings of the impurity levels due to the interaction with the magnetic moments of the nuclei. To our knowledge, no such high-pressure experiments have been made, so far.

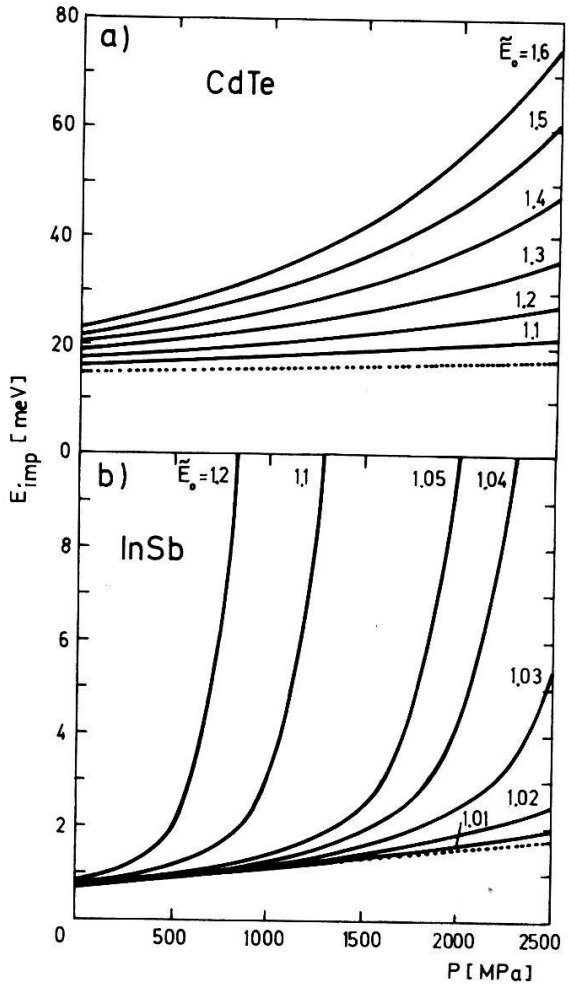

Fig.8. Pressure dependence of the ground-state energy for donors with various "initial chemical shifts" $\tilde{E}_o$. The dotted lines correspond to hydrogenic-like states /$\tilde{E}_o$=1/.

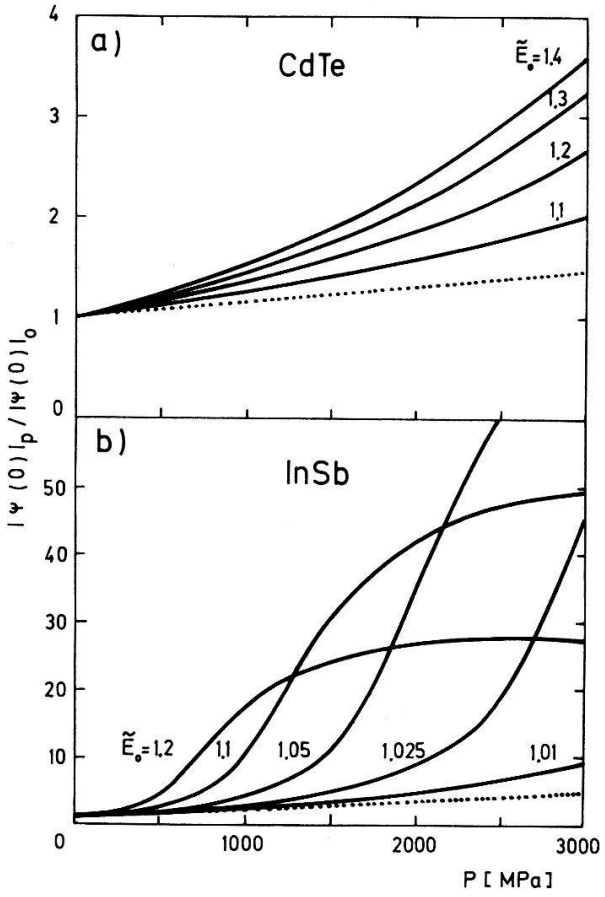

Fig.9. Pressure dependence of the wave function at $\vec{r}$=0. Note the nonmonotonic dependence on $\tilde{E}_o$ in InSb and the large magnitude of the changes. The dotted lines are for $\tilde{E}_o$=1.

4. The effect of pressure on impurity states coupled to the lattice.

Up to now we have discussed purely electronic impurity states. In the commonly adopted adiabatic approximation the lattice vibrations produce a static potential, acting on electrons. However, in case of the strong electron -phonon interaction, different electronic states may be accompanied by different lattice deformations. One-electron picture for impurity states is then inadequate and the total energy of the system "electron plus the lattice" is described in the simplest way on the configuration-coordinate diagrams [18,19] Two common versions of such diagrams are presented on Fig.10. The parabolas corresponding to two electronic states /I and II/ may not only have different equilibrium coordinates /linear coupling/ but also different phonon frequen-

cies /quadratic coupling/. All parameters of the diagrams may change with pressure.

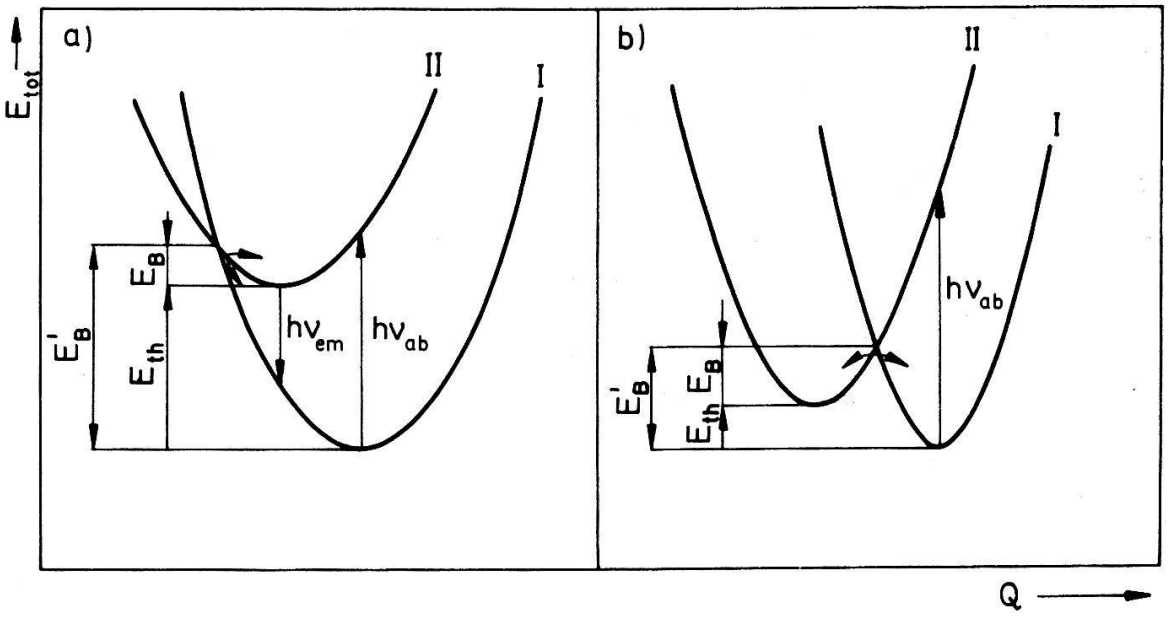

Fig.10. Total energy of the impurity versus Q for two electronic states and weak /a/ and strong /b/ coupling to the lattice. Possible optical transitions are marked with arrows. The barriers for capture and emission are denoted by E_B and E_B' /their difference is the thermal ionisation energy E_{th}/.

The experimental indication for strong impurity-lattice coupling is the thermal broadening of the optical spectra and the difference between the thermal and optical ionisation energies. In case when I or II is the band state, we may observe the thermally activated carrier capture across the energy barrier E_B' or E_B, respectively. The opposite transitions lead to the thermally activated carrier emission. The height of the barriers can be changed by the application of pressure [20].

The configuration-coordinate diagram shown on Fig.10a /encountered in alkali-halides and many semiconductors [10,21]/ leads to the Stokes shift between the absorption and emission spectra. The states I and II are often the atomic-like levels split by the crystal field. Hydrostatic pressure increases such splittings /see e.g. the optical measurements in ZnS [11,22] and in CdTe [10]/.

Much more exciting pressure effects may arise in the case shown on Fig.10b. The large separation of the equilibrium coordinates for I and II leads to the lack of radiative transitions II→I and to the possibility of metastable /non-equilibrium/ occupation of the levels I or II. In case when one

of them is a band state this results in a phenomenon of persistent photoconductivity [23]. Metastabilities introduce the time-dependences of various effects which can be studied experimentally. Shifting the levels by the hydrostatic pressure yields many interesting experimental possibilities. Let us illustrate this point with two examples.

4.1 CdTe:Cl

At ambient pressure the Cl level is degenerate with the conduction band and at low temperatures its occupation is metastable. This suggests that we have the situation shown on Fig.10b with I being the delocalized conduction band state and II being the localized impurity level. With the increasing pressure this level moves down into the gap [23,24].The pressure dependence of the free-carrier concentration [23] provides the following value of the thermal ionisation energy at T=295 K

$$E_{th}(p) = 0.08 - 15 \cdot 10^{-5} p \quad , \qquad (5)$$

where the energy is measured in eV, the pressure in MPa. The optical ionisation energy E_{opt} turns out to be much higher /around 1 eV/ and also strongly pressure-dependent. This is shown on Fig.11 where we present the edges of persistent photoconductivity measured at various pressures [23]. Dotted lines are

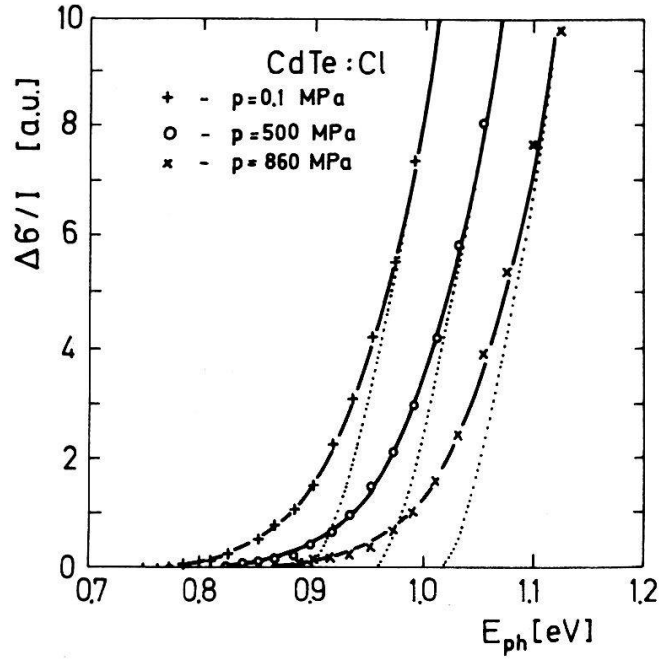

Fig.11. Persistent photoconductivity edges in CdTe:Cl at various pressures /see the text/.

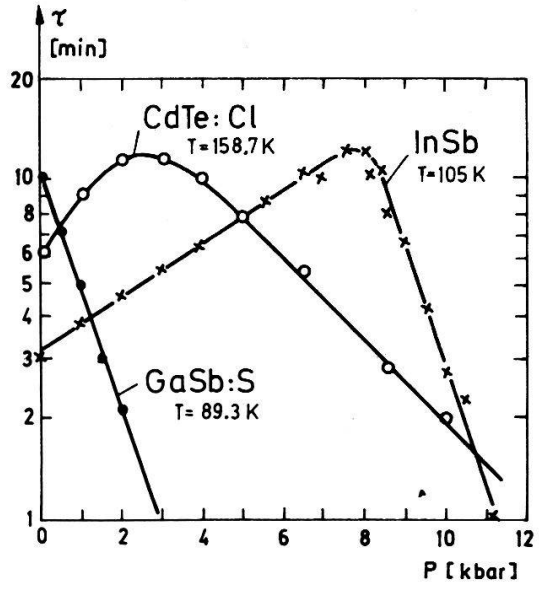

Fig.12. Relaxation time for the metastable occupation decay of impurity levels /maximum occurs when E_{th}= 0, see Sec.4.2/.

the theoretical curves obtained for purely electronic photoionisation transitions. Solid lines represent the theory taking into account the vibrational broadening of the optical spectra. This broadening is characterized by the parameter Γ which can be related to the parameters of the configuration-coordinate diagram [19].

The localized Cl level can be filled up with electrons during cool-down cycle under high-pressure. After the release of the pressure the level will still be occupied in a metastable way. Analysis of the kinetics of its decay reveals that it is exponential with the relaxation time τ strongly pressure-dependent /Fig.12/. Kinetic equations allow us to relate τ to the electron capture cross-section σ and the emission rate α /see Ref.20/. Both of these quantities turn out to be thermally activated, i.e.

$$\sigma = \sigma_\infty \cdot \exp\left[\frac{-E_B^o - (\partial E_B/\partial p)\, p}{kT}\right] , \qquad (6)$$

with $\sigma_\infty = 1.5\cdot10^{-13}\mathrm{cm}^2$, the barrier height at p=0 E_B^o=0.48eV, and the pressure coefficient of the barrier $\partial E_B/\partial p = -4\cdot10^{-5}$eV/MPa. The expression for α has the same form, with the barrier height differing from E_B by E_{th}, given by 5 . The strong pressure dependence of the barriers for capture and emission occurs in many semiconductors. In GaSb:S at about 200MPa E_B vanishes so that both the thermally activated capture and persistent photoconductivity disappear.

The experimental determination of E_{th}, E_{opt}, Γ, and E_B enables us to construct the one-dimensional configuration-coordinate diagram for Cl impurity in CdTe like the one shown on Fig.10b. However, this simple version of the diagram turns out to be insufficient to describe properly all the observed effects /e.g. lack of tunnelling through the barrier/.

4.2 Extrinsic InSb

In the purest available samples of InSb some unknown impurity /most probably oxygen/ introduces three various states [5,13,25,26]: shallow, hydrogenic-like levels /usually observed in high magnetic fields/ and two deep levels with the thermal ionisation energies given by

$$E^A = 0.085 - 10.5\cdot10^{-5}p , \qquad (7)$$

$$E^B = 0.140 - 20\cdot10^{-5}p , \qquad (8)$$

where the energy is measured in eV, the pressure in MPa. Only thelevel B exhi-

bits metastability characteristic for strong coupling to the lattice. The level A /L-like state mentioned in Sec.3.1/ has equal optical [5] and thermal [11] ionisation energies which means that it does not couple to the lattice /it is probably less localized than the level B/. Therefore the configuration coordinate diagram for this case may have the form shown on Fig.13. If, under high pressure, the crystal is cooled, most electrons will be trapped by the B state and /at low temperatures/ will remain there after the pressure release. Therefore we may regulate the free-carrier concentration by applying various pressures P_c during the cool-down cycle /this does not lower the mobility like compensating/. The n(p) dependence at T=77K obtained from the Hall effect for three different cool-down pressures is shown on Fig.14 [25]. At such low temperatures the A level is the only active trapping center but its concentration depends on the occupation of the level B, as they exclude each other.

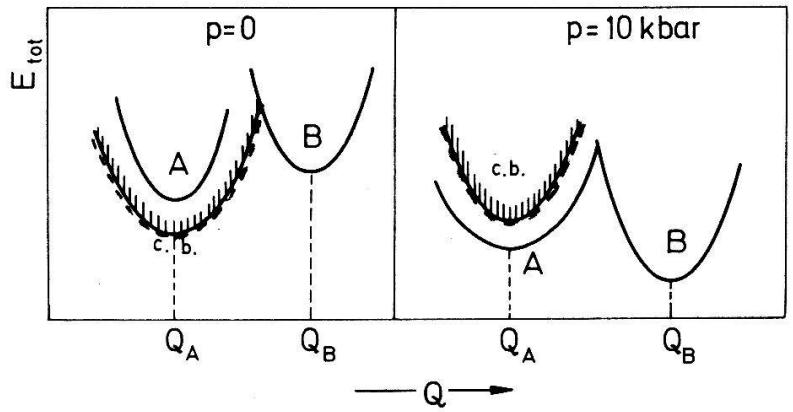

Fig.13 Configuration-coordinate diagram for InSb:0 at two pressures. Broken line denotes the hydrogenic-like level.

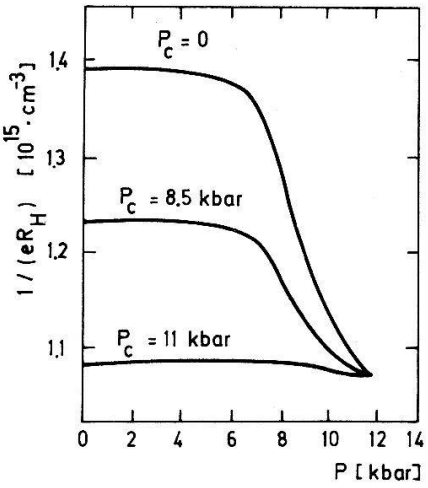

Fig.14 Free-carrier concentration versus pressure in InSb:0 for various cool-down pressures P_c.

The decay of the metastable occupation of the level B was measured at temperatures between 95K and 108K [20] /at T=77K the relaxation time for the free-carrier concentration equals 270 days!/. The $\tau(p)$ dependence is shown on Fig.12. The maximum value of τ occurs when $E_{th} \approx 0$ i.e. when the resonant level merges into the gap. The same rule holds for CdTe:Cl and GaSb:S because it follows directly from the analysis of the kinetics of I⇌II transitions.

The electron capture cross-section σ and the emission rate α may be obtained from the values of τ [20] and again they can be described by Eq.6

with $\sigma_\infty = 3 \cdot 10^{-13} cm^2$, $E_B^o = 0.413eV$, $\partial E_B/\partial p = -18 \cdot 10^{-5} eV/MPa$, $\alpha_\infty = 3.5 \cdot 10^{11} s^{-1}$. The strong pressure dependence of the capture cross-section may lead to drastic changes of the lifetime of interband photoconductivity with pressure, in the case when the defect level is a recombination center [27].

The simple configuration-coordinate diagram shown on Fig.13 does not account for some of the observed properties of the B level, namely the lack of tunnelling accross the barriers and the lack of persistent photoconductivity. A possible explanation of these facts might be supplied by the diagram shown on Fig.15, where the adiabatic potential is assumed to have two minima /they may, for instance, correspond to two equilibrium positions of a vacancy close to the oxygen impurity/. Large separation between Q_A and Q_B would be the reason for the lack of tunnelling. The energy barrier might be large but still the thermal broadening of the optical transitions B ≒ c.b. would be small and there would be no persistent photoconductivity. Still, there is too little experimental information to determine the detailed features of the configuration coordinate diagram.

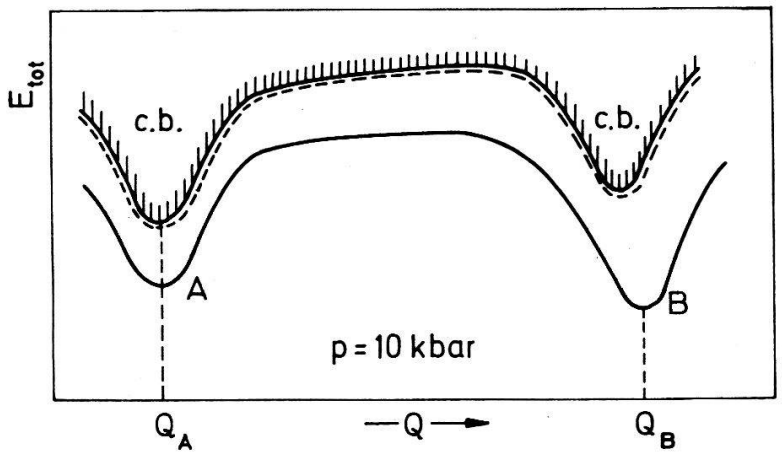

Fig.15. Alternative version of the configuration-coordinate model for InSb:O.

5. Conclusions

High pressure is a very useful tool for investigating impurity states in semiconductors as it provides much information both on the degree of localization of the state and its coupling to the lattice.

The above-described effects like the pressure-induced Mott transition, changing the resonant level into a true bound state, regulating the free carrier concentration by high-pressure freeze-out etc, are very exciting both from the theoretical and experimental point of view. Some of the pressure induced effects may be utilized in practical applications /pressure gauges, tunable infrared light sources and detectors etc/.

REFERENCES

1 W. Bujnowski, S. Porowski, and A.I. Laisaar, Prib.i Tekh.Eksper.1, 224 /197
2 G.J. Piermarini and S. Block, Rev.Sci.Instr. 46, 33 /1975/
3 B. Welber, Rev.Sci.Instr. 47, 183 /1976/
4 W. Trzeciakowski, J. Krupski, Sol.St.Comm. 44, 1491 /1982/
5 Z. Wasilewski, A.M. Davidson, and R.A. Stradling, Proc.XVI Int.Conf.Phys. o Semiconductors, Montpellier /1982/
6 I. Gorczyca, phys.st.sol./b/ 112, 97 /1982/
7 W. Paul, Proc.IX Int.Conf.Phys. of Semiconductors /Nauka,Leningrad 1969/p.1
8 L. Kończewicz and W.Trzeciakowski, phys.st.sol./b/ 115, 359 /1983/
9 P. Bogusławski and J. Mycielski, J.Phys.C 13, 1019 /1980/
10 W. Seifert, M.Sc. Thesis, Unipress, Warsaw /1975/
11 T. Koda, S. Shionoya, M. Ichikawa, and S. Minomura, J.Phys.Chem.Sol. 27, 1577 /1966/
12 J.L. Robert, A. Raymond, R.L. Aulombard, C. Bousquet, Phil.Mag.B42, 1003/19
13 S. Porowski, L. Kończewicz, M. Kończykowski, R. Aulombard, and J.L. Robert Proc.XV Int.Conf.Phys. of Semiconductors /Kyoto 1980/p.271
14 J. Callaway, "Quantum Theory of the Solid State", part II /1974/
15 W. Jantsch, K. Wunstel, O. Kumagai, and P. Vogl, Proc.XVI Int.Conf.Phys. of Semiconductors /Montpellier 1982/
16 W.Y. Hsu, J.D. Dow, D.J. Wolford, and B.G. Streetman, Phys.Rev.B16,1597/197
17 H.P. Hjalmarson, P. Vogl, D.J. Wolford, J.D. Dow, Phys.Rev.Lett.44,810/1980
18 D.L. Dexter, Sol.St.Phys. 6, 353 /1958/
19 J.M. Langer, Lecture Notes in Physics /Springer-Verlag/ 122, 123 /1980/
20 L. Dmowski, M. Baj, P. Ioannides, and R. Piotrzkowski,Phys.RevB26,4495/1982
21 C.H. Henry and D.V. Lang, Phys.Rev.B 15, 989 /1977/
22 C.S. Kelley, Journ. of Chem.Phys. 59, 5737 /1973/
23 M. Baj, Ph.D. Thesis, Warsaw University /1979/
24 M. Baj, L. Dmowski, M. Kończykowski, and S. Porowski, phys.st.sol./a/ 33, 421 /1976/
25 S. Porowski, M. Kończykowski, J. Chroboczek, phys.st.sol./b/63, 291/1974/
26 L. Dmowski, M. Kończykowski, R. Piotrzkowski, and S. Porowski, phys.st.sol./b/ K131 /1976/
27 R. Piotrzkowski, "Physics of Semiconducting Compounds",/Ossolineum 1981/, ed. J.M. Langer, p.120